



Two Step and Regression Re-aging Heat Treatment of Al-5.2%Zn-2.3%Mg Alloy Applied in Cigarette Making Machines

Hao Wang^{1*}, Jianbo Zhan¹, Zhenhua Yu¹, Jiang Yu¹, Yafeng Ji², Ying Zhang¹,
Tao Wang¹, Yao Yu¹, Muyan Li³, Danfeng He⁴, Hongkui Zhang⁵, Rongrong Fu⁶,
Na Zan⁷, Wei Ding¹, Liwei Li¹, Liang Cheng¹, Baoshan Yue¹, Han Zheng¹,
Zhiqiang Li¹ and Li Gao¹

¹Technical Center for China Tobacco Yunnan Industrial Co., Ltd., Kunming 650231, P. R. China.

²Heavy Industry Engineering Center of China Ministry of Education, Taiyuan University of Science and Technology, Taiyuan 030024, P. R. China.

³Honghe Cigarette Factory, Hongyunhonghe Tobacco (Group) Co. Ltd., Honghe 652399, China.

⁴Qvjing Cigarette Factory, Hongyunhonghe Tobacco (Group) Co. Ltd., Qujing 655001, Yunnan, China.

⁵Fushun Branch of China Coal Research Institute, Fushun 113001, P. R. China.

⁶Measurement Technology and Instrumentation Key Laboratory of Hebei Province, Yanshan University, Qinhuangdao 066004, P. R. China.

⁷Design and Research Center, AVIC Commercial Aircraft Engine Co. Ltd. Shanghai 200241, P. R. China.

Authors' contributions

This work was carried out in collaboration between all authors. Author HW designed the study, performed the statistical analysis, wrote the protocol and wrote the first draft of the manuscript. Authors JZ, ZY, JY, YJ, YZ, TW, YY, ML, DH, HZ, RF and NZ managed the analyses of the study. Authors WD, LL, LC, BY, HZ, ZL and LG managed the literature searches. All authors read and approved the final manuscript.

Article Information

DOI: 10.9734/ACSJ/2016/26486

Editor(s):

(1) Ling Bing Kong, School of Materials Science and Engineering, Nanyang Technological University, Singapore.

Reviewers:

(1) Haider Tawfiq Naeem Alhajobeed, Almuthanna University, Iraq.

(2) Avijit Sinha, Dalhousie University, Canada.

Complete Peer review History: <http://sciencedomain.org/review-history/14635>

Original Research Article

Received 20th April 2016
Accepted 7th May 2016
Published 14th May 2016

ABSTRACT

Deformation scheme and pre-heat treatment of Al-5.2%Zn-2.3%Mg aluminum alloy is chosen, homogenizing annealing at 415°C for 1h, cooling to 200°C in furnace at a cooling rate of less than 30°C/h and then cooling to room temperature to make Al-5.2%Zn-2.3%Mg aluminum alloy annealed fully. Heat treatment tests of Al-5.2%Zn-2.3%Mg aluminum alloy mainly consisting of rolling and aging were conducted, and the optimum peak aging mechanism is 120°C/20 h. Through comparison of microstructure and mechanical properties with different deformation and aging mechanism, effect of deformation rates and aging mechanism on properties of Al-5.2%Zn-2.3%Mg aluminum alloy was analyzed, and optimum double-peak aging mechanism is 110°C/7h+170°C/16 h. Orthogonal experiments were carried out to analyze mechanical and electrical properties of tested materials before and after deformation, and effect of aging mechanism on Al-5.2%Zn-2.3%Mg Al alloy was analyzed, and the optimum regression aging mechanism is 120°C/20 h+170°C/40 min+120°C/20 h.

Keywords: Al-5.2%Zn-2.3%Mg alloy; heat treatment; aging; mechanical properties; cigarette making machine.

1. INTRODUCTION

Al-Zn-Mg-Cu aluminum alloys belong to superduralumin, which possesses high strength at room temperature [1-3]. High content of Zn in the alloy has a high solubility in aluminum and abnormal precipitation hardening effect, which makes the strength and fracture toughness improved, and having a good hot workability, but with lower ductility and a tendency to stress corrosion. Al-Zn-Mg-Cu aluminum alloys have high strength and good hardenability, which is suitable for the production of pre-stretching board, large-size extrusion products, large forgings, and the magnetic properties similar to electrical steel which makes it widely used in aerospace and military industries [4-7]. In the different parts of cigarette machines, including rod forming machine, tobacco feeding machine, cutting machine and manipulator all have detecting devices made of Al-Zn-Mg alloy.

In order to develop aluminum alloy with high strength, high toughness and high resistance to stress corrosion cracking, many trials and studies were carried out for decades, and there are mainly two effective methods, TMT (Thermo-Mechanical treatment) and RRA (Retrosession and Re-ageing) [8-12]. TMT is a process combining both strain hardening after the plastic deformation and phase transformation strengthening after heat treatment [13-16]. The basic principle is to increase the density of defects in the metal deformation and change its distribution, deformation defects generated by phase transition during heat treatment will affect nucleation and distribution of the new phases, at the same time, the formation of new phases will pin or block movement of dislocations defects,

making defects stable and microstructure refine, improving its strength and toughness [17-21]. Dislocation imported by deformation often combined into a dislocation network through slipping or climbing movement to reduce energy, therefore, the microstructure of the treated Al-Zn-Mg aluminum alloy is high dislocation density and sub-structures, and thermo-mechanical treatment is essentially substructure strengthening [21-26].

In 1974 B.M.Cina first proposed that after artificial aging is suitable for regression treatment, and later repeating the original artificial aging, which would effectively improve mechanical properties and corrosion resistance of aluminum alloy, and the heat treatment process is called RRA treatment [20]. Through peak aging, tensile strength of alloy could achieve ideal value, but the corrosion resistance decreases. In RRA, the temperature and time of second two-step aging is critical to the whole aging process. However, to the best of authors' knowledge, there have been few reports on deformation and ageing treatment of Al-5.2%Zn-2.3%Mg aluminum alloy. The purpose of the present study is to study the effect of the deformation and different ageing treatment on the microstructure and mechanical properties of Al-5.2%Zn-2.3%Mg aluminum alloy, providing reference for its various industrial applications such as in cigarette making machines.

2. EXPERIMENTAL MATERIALS AND METHODS

2.1 Experimental Materials

The materials used in this research work were wrought heat treatable Al-5.2%Zn-2.3%Mg

aluminum alloy, and the chemical compositions are given in Table 1.

2.2 Thermal Analysis

DSC thermal analysis is conducted in the EPM laboratory of Northeastern University with MDSCQ100 heat analyzer, samples are selected as a bulk sample of 5 mm side length cleaned with alcohol and acetone, respectively before the test, with pure aluminum as a reference. The heating rate is 10°C/min, and the temperature range is between 300°C~ 550°C.

2.3 Homogenization Treatment

Annealing temperature was selected as 415°C for 1h, and the plate was cooled to less than 200°C with a air furnace cooling rate of 30°C/h and then air cooled to room temperature.

2.4 Rolling

The slab after homogenization at 450°C is rolled from 40 mm at 470°C to 10.4 mm (total deformation ratio of 79%), during which deformation ratio of 30%, 50%, 70% were achieved, and the slab was rolled by single pass cold rolling. After solid solution at 475°C for 1h the slab was quenched immediately, and then it was cold-rolled to 2.8 mm sheet (deformation ratio of 73%) at room temperature for the subsequent experiments, and the media of cooling after the aging treatment is air.

2.5 Aging

After rolling and solution, the alloy was subjected to aging treatment immediately, and aging

treatment is divided into peak aging, two-step aging and RRA in this experiment. For peak aging the aging temperature was selected as 110°C, 120°C and 130°C with aging time of 4 h, 8 h and 12 h to determine the optimum aging temperature. Then the optimum temperature aging time was selected from 4 h, 8 h, 12 h, 16 h, 20 h and 24 h at the optimum aging temperature. Two-step aging temperature and time range was selected as 95°C ~125°C for 4 h ~10 h in the first stage, 170°C ~200°C for 14 h ~20 h in the second stage, as shown in Table 2.

According to the experimental features of both peak aging parameters and RRA treatment, the second aging temperature was selected as 170°C and 210°C, and the aging time is 20 min, 40 min, 60 min, respectively. The specific RRA trial program is shown in Table 3.

2.6 Hardness, Conductivity Test

Hardness experiments were carried out by using 430/450SVDTM Vickers hardness measurement instrument with a load of 49N for a dwell time of 15 s. FD102 digital eddy current conductivity meter with an accuracy of $\pm 0.1\%$ ACS was applied in conductivity measurement. The tensile specimens were got parallel to the rolling direction.

2.7 Microstructure Observation

OLYMPUS DP70 inverted metallurgical microscope is used to observe the microstructure of the alloy after different alloy. SSX-550 scanning electron microscope with a resolution of 3.5nm particles is applied for analyzing certain surface and elements in the dimples with supporting spectrum analyzer.

Table 1. Chemical compositions of Al-5.2%Zn-2.3%Mg aluminum alloy (mass, %)

Elements	Zn	Mg	Cu	Fe	Si	Mn	Zr	Ti	Al
Mass, %	5.2	2.3	2.3	0.15	0.12	0.1	0.12	0.06	Bal

Table 2. Selection of levels in two-step aging orthogonal design

Level	First two-step aging temperature/°C	First two-step aging time/h	Second two-step aging temperature /°C	Second two-step aging time /h
1	95	4	170	14
2	105	6	180	16
3	115	8	190	18
4	125	10	200	20

Table 3. Design of RRA tests

No.	1 st two-step aging temperature/°C	1 st two-step aging time/h	2 nd two-step aging temperature/°C	2 nd two-step aging time/min	3 rd two-step aging temperature/°C	3 rd two-step aging time /h
1	120	20	170	20	120	20
2	120	20	170	40	120	20
3	120	20	170	60	120	20
4	120	20	210	20	120	20
5	120	20	210	40	120	20
6	120	20	210	60	120	20

3. RESULTS AND DISCUSSION

3.1 Determination of Solution Temperature

Differential scanning calorimetry curve (DSC curve) is a technique of measurement for the energy changes between the sample and the reference material with variation of temperature and time. The curve is based on the endothermic and exothermic phenomena accompanied by the physical and chemical changes occurred in the heating process. At the program-controlled temperature, the function relationship of heat flow rate variation with temperatures was measured, which is commonly used to quantitatively measure melting point and hot-melt. From Fig. 1 we could find that the solution temperature is 480°C (10°C lower than the melting point).

3.2 Effect of Homogenization on Microstructure

As can be seen in Fig. 2, in the original state of microstructure there are many precipitates with uneven size, and the amount significantly reduced after homogenization, also the microstructure has been refined to a certain extent. This is due to the increase of solute

atoms solubility in the matrix during the homogenization process, therefore, the precipitates continuously dissolve into the matrix, and the remaining precipitates diminish.

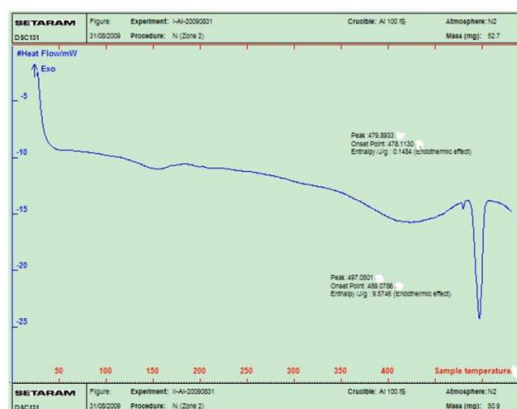


Fig. 1. DSC curve of Al-5.2%Zn-2.3%Mg alloy

The same time, due to the diffusion of solute elements, the microstructure tends to be uniform, which is beneficial to the following uniform rolling process. As can be seen in Fig. 3(b), the precipitate is still not complete solid solution in the matrix, the solution treatment of the alloy after hot rolling is necessary.

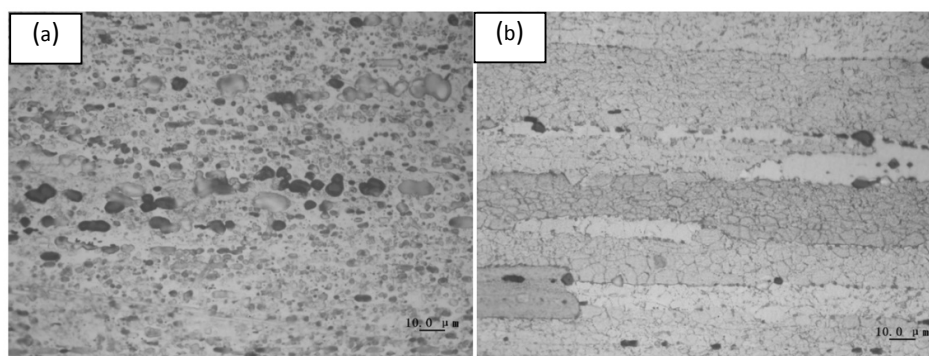


Fig. 2. Microstructure of alloys before and after homogenization (a) Before homogenization, (b) After homogenization

After homogenization, the matrix is also scanned, Fig. 3 and Table 4 show the elements construction in the matrix, and the main solute elements are Zn and Mg. Combining phase characteristics, we could infer that the black precipitates is $\eta(\text{MgZn}_2)$ 、 $\text{S}(\text{CuMgAl}_2)$ and $\text{T}(\text{AlZnMgCu})$. Binary crystal containing T (AlZnMgCu) and $\alpha(\text{Al})$ form is porous-intensive, and T (AlZnMgCu) shows dark gray. Crystal S (CuMgAl_2) and $\alpha(\text{Al})$ of the formed is honeycomb.

Table 4. Elements of composition after matrix's scanning

Element	Mass (wt%)	At (a%)
Zn	6.44	2.76
Mg	2.75	3.16
Al	90.81	94.09

3.3 Effect of Deformation on Properties of Alloy

To study the deformation ratio on the properties of alloy performance, different reduction ratios were conducted and both hardness testing and microstructure observation were carried out. As shown in Table 5, after cold rolling the hardness of alloy increased apparently, especially to initial status.

As shown in Fig. 4, microstructure contrast of alloy with different reduction ratios shows that with the increase of the deformation rate the grain sizes become smaller and their distribution is more uniform, also the precipitates in the grains increase.

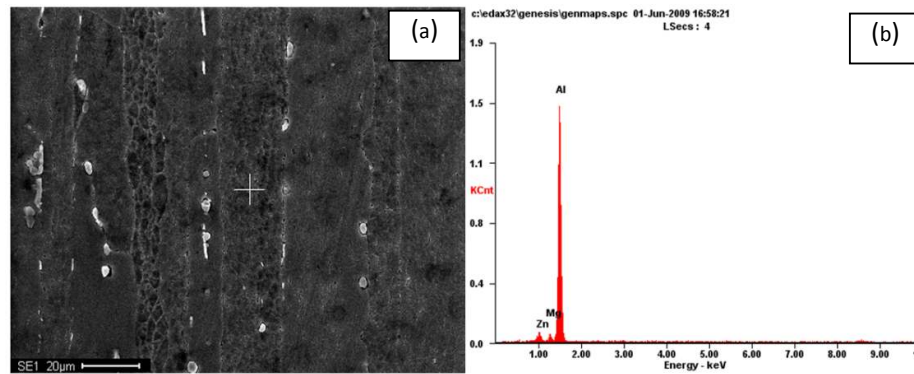


Fig. 3. Composition scanning of matrix after homogenization

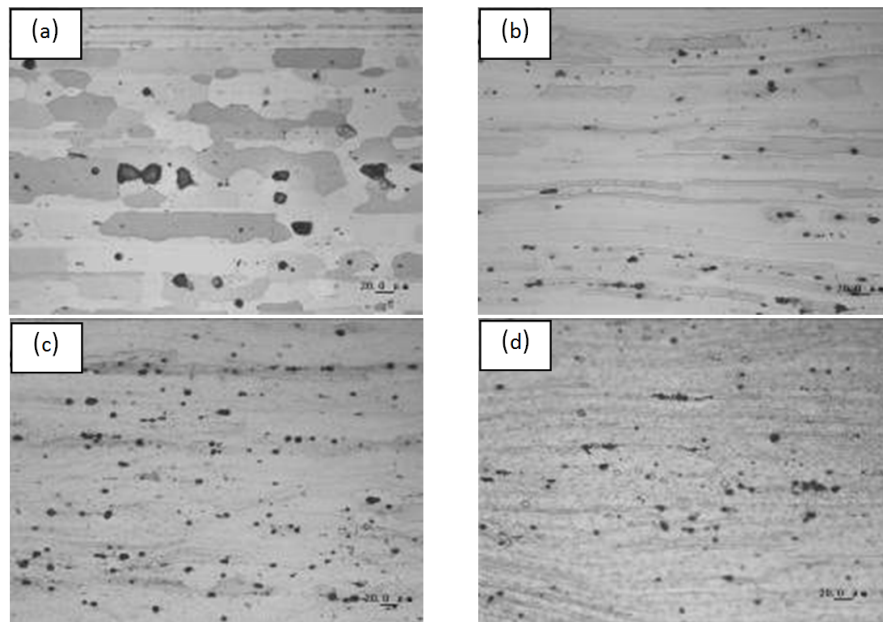


Fig. 4. Comparison of microstructure of alloys after different deformation ratio(a)without deformation, (b)30%, (c)50%, (d)70%

3.4 Peak Aging

Mechanical properties after peak aging test at 110°C, 120°C, 130°C for 4 h, 8 h and 12 h are shown in Table 6. Variations of properties appear at three different aging temperatures. Mechanical properties of alloy aged at 120°C is better than 110°C and 130°C. Therefore, peak aging temperature of alloy is settled as 120°C.

Mechanical properties of alloy with different aging time at 120°C are shown in Table 7. The tensile strength and yield strength fluctuate with the rise of peak aging time, and arriving at peak value after aging for 20 h and medium in elongation, but highest in conductivity. As discussed above, the optimum peak aging parameter is determined as 120°C for 20 h.

Microstructure of alloy after peak aging was observed, which is as shown in Fig. 5. Initial coarse grains in the alloy gradually refine and

arrive at finest status after aging for 20h. As the aging time increased after peak aging time, the grain sizes grow further, the grains become coarse again, which also explains why the alloy reached the highest hardness value at the peak aging time of 20 h.

Aging hardening appears in aluminum alloy. As the aging temperature and aging time ascend, the alloy strength ascends gradually and declines after the peak aging process. Aging intensity variation is mainly caused by three factors: (1) solid solution strengthening; (2) substrate's recovery and recrystallization; (3) new phase precipitation [15-19]. Both factors could make strength decrease as the aging time decreases, while the third factor makes the strength increase, but the strength will descend when the coherent relationship of precipitation phase and the parent phase is destroyed and the precipitated phases become coarse [17-18,22].

Table 5. Hardness of alloy before and after different deformation

Treatment	Initial status	After homogenization	30% cold-rolling	50% cold-rolling	70% cold-rolling
Hardness(HV)	91.6	100.7	106.2	113.2	120.2

Table 6. Mechanical properties of alloy at different peak aging temperature

Aging temperature/time	Tensile strength /MPa	Yield strength /MPa	Elongation / %
110°C/4 h	425.7	367.5	5.6
110°C/8 h	466.6	406.4	5.9
110°C/12 h	471.0	418.3	6.6
120°C/4 h	432.7	387.5	7.7
120°C/8 h	489.2	429.8	7.3
120°C/12 h	508.7	441.2	6.2
130°C/4 h	427.5	359.2	5.5
130°C/8 h	453.8	389.9	7.1
130°C/12 h	487.6	434.6	6.1

Table 7. Mechanical properties of alloy aged at 120°C for different aging time

Peak aging time /h	Tensile strength /MPa	Yield strength /MPa	Elongation /%	Hardness /HV	Conductivity / %IACS
0	392.6	328.0	5.5	120.2	28.8
4	432.7	387.5	7.7	125.6	30.0
8	489.2	429.8	7.3	132.5	31.9
12	508.7	441.2	6.2	136.8	33.4
16	505.4	455.6	6.9	139.0	33.3
20	546.1	483.3	7.2	160.7	34.8
24	538.9	458.2	7.6	149.2	35.0

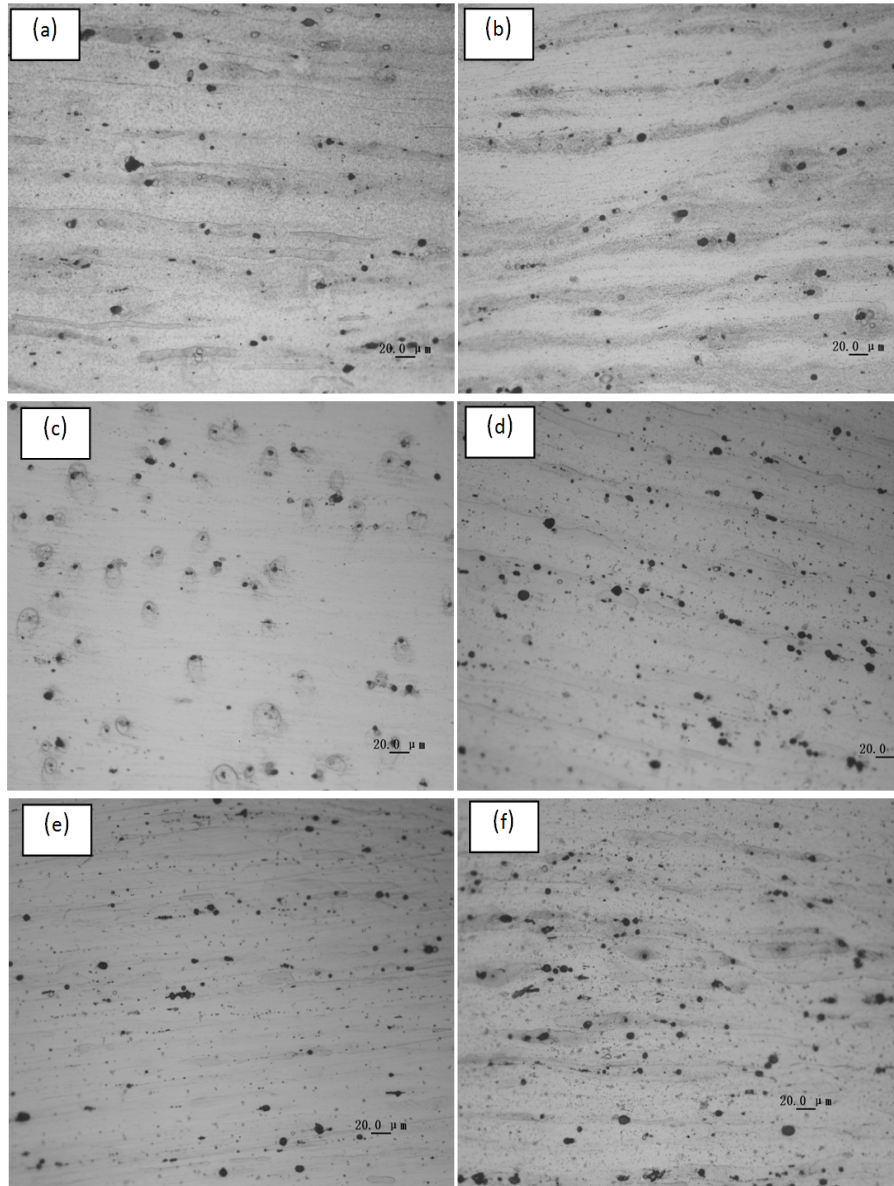


Fig. 5. Effects of different aging time on alloys' microstructure at 120°C(a) 4 h, (b) 8 h, (c) 12 h, (d)16 h, (e)20 h, (f)24 h

3.5 Two-step Aging Test Results

After stage aged aluminum alloy performance test results with four influencing factors are shown in Table 9. The maximum tensile strength is 558.7 MPa, while the minimum is 449.7 MPa, and the gap between them is 109 MPa, which signifies that the effect of different influencing factors on tensile strength is apparent. The yield strength and elongation also show such apparent influence. Different influencing factors have some

effect on both hardness and conductivity. For conductivity, the maximum conductivity is 37.2% IACS and the minimum is 26.8% IACS with a difference of 10.4% IACS.

In this paper we use the consolidated balance multi-index method, range analysis of each indicator in turn, then finding a more satisfactory level combination. The effect of first two-step aging temperature on mechanical properties is significant [23]. There is some variation in tensile

strength and yield strength, and elongation at 105°C and 115°C is relatively higher, therefore, the optimum first two-step aging temperature is 110°C. 6 h or 8 h is more appropriate for first two-step aging time to ensure better mechanical properties. Through range analysis, secondary aging temperature is extremely significant to mechanical properties among four influencing factors. Indicating that in the stabilization stage, the aging temperature is essential to mechanical properties. At 170°C strength, elongation and hardness could be guaranteed, while at 180°C the alloy shows a worse conductivity. Therefore, 170°C is chosen as optimum second two-step aging temperature. The alloy achieves optimum mechanical properties for second two-step aging time of 16h. Overall, optimum two-step aging process is 110°C/7 h + 170°C/16 h.

Through verification by experiment, after two-step aging 110°C/7 h + 170°C/16 h, the alloy's

mechanical properties are as follows tensile strength 567.7MPa, yield strength 503.6MPa, elongation 13.5%, the hardness 172.3 HV, conductivity 39.6% IACS. The test results show that the orthogonal design is reasonable and appropriate.

3.6 RRA Treatment

While the second two-step aging temperature is selected at 170°C, tensile strength and yield strength achieved the maximum value. Elongation reaches a good level after aging for 40min. A combination of comprehensive properties as follows could be achieved after the second stage of RRA is 170°C/40 min, tensile strength 588.4 MPa, yield strength 539.2 MPa, elongation 15.6%, hardness 182.1 HV, conductivity 47.9% IACS.

Table 9. Results of two-step aging orthogonal tests

No.	A	B	C	D	Tensile strength /MPa	Yield strength /MPa	Elongation /%	Hardness /HV	Conductivity /%IACS
1	1	1	1	1	527.8	470.4	9.1	155.8	26.8
2	1	2	2	2	532.6	481.7	7.9	163.9	27.5
3	1	3	3	3	473.9	427.0	7.3	134.1	29.0
4	1	4	4	4	456.3	418.7	8.9	133.4	32.3
5	2	1	2	3	481.1	430.6	8.0	141.6	27.4
6	2	2	1	4	558.7	473.9	11.3	166.3	26.3
7	2	3	4	1	504.3	460.1	9.5	152.1	29.2
8	2	4	3	2	500.6	459.2	8.5	149.9	29.3
9	3	1	3	4	449.7	397.5	10.8	129.8	31.1
10	3	2	4	3	492.2	455.3	8.3	146.0	31.7
11	3	3	1	2	530.4	478.1	10.3	163.7	37.2
12	3	4	2	1	537.4	476.0	10.4	166.2	29.3
13	4	1	4	2	460.8	408.8	7.2	134.9	32.8
14	4	2	3	1	535.7	472.2	9.1	165.3	30.5
15	4	3	2	4	495.3	449.6	10.3	147.6	28.1
16	4	4	1	3	541.2	485.1	8.1	168.2	29.9

Table 10. Results of RRA tests

No.	Tensile strength /MPa	Yield strength /MPa	Elongation /%	Hardness /HV	Conductivity %IACS
1	532.1	484.6	13.3	143.5	45.6
2	588.4	539.2	15.6	182.1	47.9
3	550.9	512.7	16.7	169.4	48.8
4	491.0	455.8	14.9	123.8	43.2
5	534.7	491.5	17.1	142.0	44.0
6	519.3	468.1	15.4	147.6	45.1

4. CONCLUSIONS

Orthogonal experiment was applied in analyzing mechanical and electrical properties, and aging process at certain deformation treatment of alloy was settled, which provides reference for various applications of alloy for future industry. The conclusions are as follows:

- (1) Deformation scheme and pre-heat treatment of Al-5.2%Zn-2.3%Mg aluminum alloy is chosen, homogenizing annealing at 415°C for 1 h, cooling to 200°C in furnace at a cooling rate of less than 30°C/h and then cooling to room temperature to make alloy fully annealed. Solid solution temperature of Al-5.2%Zn-2.3%Mg aluminum alloy is 480°C. Feasible rolling process is that the alloy is hot-rolled at 470°C from 40 mm to 10.4 mm, and then immediately solid solution at 475°C for 1 h, then cold-rolled to 2.8 mm sheet at room temperature.
- (2) After tested deformation, the optimum peak aging process of Al-5.2%Zn-2.3%Mg aluminum alloy is determined: 120°C/20 h. Properties are as follows after above peak aging process: Tensile strength 546.1 MPa, yield strength 483.3 MPa, elongation 7.2%, hardness 160.7 HV, conductivity 34.8% IACS. Optimum strength with low elongation was obtained after peak aging treatment.
- (3) The optimum two-step aging process of Al-5.2%Zn-2.3%Mg aluminum alloy after rolling is determined: 110°C/7 h+170°C/16 h. Properties are as follows after above two-step aging process: Tensile strength 567.7MPa, yield strength 503.6 MPa, elongation 13.5%, hardness 172.3 HV, conductivity 39.6% IACS. Both strength and elongation are improved after two-step aging.
- (4) After rolling, the optimum RRA process of Al-5.2%Zn-2.3%Mg aluminum alloy is determined:
120°C/20 h + 170°C/40 min + 120°C/20 h, Properties are as follows after above two-step aging process: Tensile strength 588.4 MPa, yield strength 539.2 MPa, elongation 15.6%, hardness 182.1 HV, conductivity 47.9% IACS. Both mechanical properties and conductivity were enhanced after RRA treatment.

COMPETING INTERESTS

Authors have declared that no competing interests exist.

REFERENCES

1. Huda Z, Edi P. Materials selection in design of structures and engines of supersonic aircrafts: A review. *Materials & Design*. 2013;47(4):552-560.
2. Naeem HT, Mohammed KS, Ahmad KR. Effect of friction stir processing on the microstructure and hardness of an aluminum-zinc-magnesium-copper alloy with nickel additives. *Physics of Metals & Metallography*. 2015;116(10):1035-1046.
3. Wang H, Li CS, Zhu T. Hard magnetization direction and its relation with magnetic permeability of highly grain-oriented electrical steel. *International Journal of Minerals Metallurgy and Materials*. 2014; 21(11):1077-1082.
4. Xu L, Dai G, Huang X, et al. Foundation and application of Al-Zn-Mg-Cu alloy flow stress constitutive equation in friction screw press die forging. *Materials & Design*. 2013; 47(5):465-472.
5. Naeem HT, Mohammad KS, Ahmad KR. The effect of microalloying of nickel, RRA treatment on microstructure and mechanical properties for high strength aluminum alloy. *Advanced Materials Research*. 2014;925:253-257.
6. Xu J, Gao ZH, Zhang ZF, et al. Application research on annular electromagnetic stirring casting process of Al-Zn-Mg-Cu alloy. *Solid State Phenomena*. 2012; 466(10):192-193.
7. Gu R, Ngan AH. Size effect on the deformation behavior of duralumin micropillars. *Scripta Materialia*. 2013; 68(11):861-864.
8. Naeem HT, Mohammad KS, Ahmad KR. Characteristics of Al-Zn-Mg-Cu alloys with nickel additives synthesized via mechanical alloying, cold compaction, and heat treatment. *Arabian Journal Forence & Engineering*. 2014;39(12):1-10.
9. Wang H, Li CS, Mei RB, et al. Effect of ball scribing on magnetic shielding efficiency of grain-oriented silicon steel. *Journal of Iron and Steel Research International*. 2014; 21(7):679-684.
10. Markushev MV. On the principles of the deformation methods of aluminum-alloys grain refinement to ultrafine size: I. Fine-

- grained alloys. The Physics of Metals and Metallography. 2009;108(1):43-49.
11. Mohammed KS, Naeem HT. Corrosion behaviour of Al₂O₃p reinforced Al-Zn-Mg-Cu-Ni-Co alloy fabricated via PM. International Journal of Science & Research. 2015;4(3):645-649.
 12. Naeem HT, Mohammad KS, Hussin K, et al. Assessment of retrogression and re-aging treatment on microstructural and mechanical properties of Al-Zn-Mg-Cu P/M alloy. International Conference on Mathematics, Engineering. 2014;1660(3): 67-68.
 13. Naeem HT, Mohammed KS. Microstructural evaluation and mechanical properties of an Al-Zn-Mg-Cu-Alloy after addition of nickel under RRA Conditions. Materials Sciences & Applications. 2013;4(11):704-711.
 14. Valiev RZ, Murashkin MY, Semenova IP. Grain boundaries and mechanical properties of ultrafine-grained metals. Metallurgical and Materials Transactions A, 2010;41(4):816-822.
 15. Marlaud T, Deschamps A, Bley F, et al. Evolution of precipitate microstructures during the retrogression and re-aging heat treatment of an Al-Zn-Mg-Cu alloy. Acta Materialia. 2010;58(14):4:814-4826.
 16. Deng Y, Yin Z, Zhao K, et al. Effects of Sc and Zr microalloying additions and aging time at 120°C on the corrosion behaviour of an Al-Zn-Mg alloy. Corrosion Science. 2012;65(12):288-298.
 17. Kverneland A, Hansen V, Thorkildsen G, et al. Transformations and structures in the Al-Zn-Mg alloy system: A diffraction study using synchrotron radiation and electron precession. Materials Science and Engineering: A. 2011;528(3):880-887.
 18. Chemingui M, Khitouni M, Jozwiak K, et al. Characterization of the mechanical properties changes in an Al-Zn-Mg alloy after a two-step ageing treatment at 70°C and 135°C. Materials & Design. 2010; 31(6):3134-3139.
 19. Liu M, Klobes B, Maier K. On the age-hardening of an Al-Zn-Mg-Cu alloy: A vacancy perspective. Scripta Materialia. 2011;64(1):21-24.
 20. Cina BM. Reducing the susceptibility of alloys, particularly aluminium alloys, to stress corrosion cracking [P] 1974-12-24 US Patent No.3,856,584.
 21. Deschamps A, Texier G, Ringeval S, et al. Influence of cooling rate on the precipitation microstructure in a medium strength Al-Zn-Mg alloy. Materials Science and Engineering: A. 2009;501(2):133-139.
 22. Wu LM, Seyring M, Rettenmayr M, et al. Characterization of precipitate evolution in an artificially aged Al-Zn-Mg-Sc-Zr alloy. Materials Science and Engineering: A. 2010;527(4-5):1068-1073.
 23. Wang H, Li CS, Li J, et al. Effect of deformation and aging on properties of Al-4.1%Cu-1.4%Mg aluminum alloy. ISRN Materials Science. 2013;902970:1-7. Available:<http://dx.doi.org/10.1155/2013/902970>
 24. Wang GS, Zhao ZH, Cui JZ, et al. Microstructure and RRA treatment of LFEC 7075 aluminum alloy extruded bars. Journal of Wuhan University of Technology-Mater. Sci. Ed. 2013; 28(1):184-191.
 25. Yuan ZS, Liu Z, Xie YH, et al. Effects of RRA treatments on microstructures and properties of a new high-strength aluminum-lithium alloy-2A97. 2007;20(2): 187-192.
 26. Bansod AR, Chimankar OP, Gandhe A, et al. Effect of Al₂O₃ Filler on Mechanical Behavior Acrylic Films. American Chemical Science Journal. 2015;5(1):26-31.

© 2016 Wang et al.; This is an Open Access article distributed under the terms of the Creative Commons Attribution License (<http://creativecommons.org/licenses/by/4.0>), which permits unrestricted use, distribution, and reproduction in any medium, provided the original work is properly cited.

Peer-review history:

The peer review history for this paper can be accessed here:

<http://sciencedomain.org/review-history/14635>